Journal of Contaminant Hydrology 138–139 (2012) 83–92

Contents lists available at SciVerse ScienceDirect

Journal of Contaminant Hydrology

journal homepage: www.elsevier.com/locate/jconhyd

Causes and implications of colloid and microorganism retention hysteresis

Scott A. Bradford [a,*], Hyunjung Kim [b]

[a] US Salinity Laboratory, USDA, ARS, Riverside, CA, USA
[b] Department of Mineral Resources and Energy Engineering, Chonbuk National University, 664-14 Duckjin, Jeonju, Jeonbuk 561-756, Republic of Korea

ARTICLE INFO

Article history:
Received 14 October 2011
Received in revised form 18 June 2012
Accepted 27 June 2012
Available online 7 July 2012

Keywords:
Microorganism
Colloid
Transport
Chemical heterogeneity
Surface roughness
Hysteresis

ABSTRACT

Experiments were designed to better understand the causes and implications of colloid and microorganism retention hysteresis with transients in solution ionic strength (IS). Saturated packed column experiments were conducted using two sizes of carboxyl modified latex (CML) microspheres (0.1 and 1.1 μm) and microorganisms (coliphage φX174 and *E. coli* D21g) under various transient solution chemistry conditions, and 360 μm Ottawa sand that was subject to different levels of cleaning, namely, a salt cleaning procedure that removed clay particles, and a salt + acid cleaning procedure that removed clay and reduced microscopic heterogeneities due to metal oxides and surface roughness. Comparison of results from the salt and salt + acid treated sand indicated that microscopic heterogeneity was a major contributor to colloid retention hysteresis. The influence of this heterogeneity increased with IS and decreasing colloid/microbe size on salt treated sand. These trends were not consistent with calculated mean interaction energies (the secondary minima), but could be explained by the size of the electrostatic zone of influence (ZOI) near microscopic heterogeneities. In particular, the depth of local minima in the interaction energy has been predicted to increase with a decrease in the ZOI when the colloid size and/or the Debye length decreased (IS increased). The adhesive interaction was therefore largely irreversible for smaller sized 0.1 μm CML colloids, whereas it was reversible for larger 1.1 μm CML colloids. Similarly, the larger *E. coli* D21g exhibited greater reversibility in retention than φX174. However, direct comparison of CML colloids and microbes was not possible due to differences in size, shape, and surface properties. Retention and release behavior of CML colloids on salt + acid treated sand was much more consistent with mean interaction energies due to reduction in microscopic heterogeneities.

1. Introduction

The interaction energy of colloids and microorganisms with mineral surfaces is commonly calculated as the sum of electrostatic and van der Waals interactions (Derjaguin and Landau, 1941; Verwey and Overbeek, 1948). Most solid surfaces are negatively charged at prevailing pH conditions (Wan and Tokunaga, 2002) and this produces an energy barrier to attachment in the primary minimum (i.e., unfavorable attachment conditions). However, adhesive interactions may still occur under unfavorable conditions as a result of a weak secondary minimum interaction at a separation distance of a few nm from the collector surface (Franchi and O'Melia, 2003; Hahn et al., 2004; Kuznar and Elimelech, 2007; Tufenkji and Elimelech, 2005). The strength of this secondary minimum increases with IS (decreasing Debye length) and the colloid size. In addition, microscopic heterogeneities may arise from surface roughness (Hoek and Agarwal, 2006) and chemical impurities such as metal oxides, organics, and hydroxyl groups on silica surfaces (Song et al., 1994; Tufenkji and Elimelech, 2005; Vaidyanathan and Tien, 1991). These heterogeneities may produce local reductions in the energy barrier height that are favorable for attachment (Duffadar and Davis, 2007, 2008; Duffadar et al., 2009; Hoek and Agarwal, 2006; Kalasin and Santore, 2008; Kozlova and Santore, 2006, 2007). When the size of the chemical heterogeneity is much larger than the diameter of the colloid-surface contact area, particle deposition

* Corresponding author. Tel.: +1 951 369 4857.
E-mail address: Scott.Bradford@ars.usda.gov (S.A. Bradford).

0169-7722/$ – see front matter © 2012 Published by Elsevier B.V.
doi:10.1016/j.jconhyd.2012.06.007

will be insensitive to changes in the solution IS (Johnson et al., 1996). Conversely, when the size of the heterogeneity is similar or smaller in size than the diameter of the colloid-surface contact area, then particle deposition will be influenced by repulsive interactions from neighboring regions that will be sensitive to the IS (Duffadar and Davis, 2008). The deposition rate decreases over time as microscopic heterogeneities are filled or "blocked" by deposited colloids (Adamczyk et al., 1994; Privman et al., 1991; Russel et al., 1989).

Hysteresis in the amount of colloid retention in porous media has recently been observed with transients in solution IS and several different explanations have been proposed (Torkzaban et al., 2010). One hypothesis was that the amount of colloid retention was dependent on the solid phase colloid mass transfer (e.g., rolling) to low velocity regions (grain-grain contacts and surface roughness locations) where the torque balance is favorable for retention (Bradford et al., 2007, 2011a; Torkzaban et al., 2007). The number of colloids that can roll to these regions is dependent on the strength of the adhesive interaction (e.g., the depth of the secondary minimum). Subsequent changes in the IS will not necessarily release colloids that are retained at grain-grain contact or surface roughness locations because of the presence of small-scale flow vortices (Taneda, 1979; Torkzaban et al., 2008). A second hypothesis was that a larger number of colloids interact with macroscopic heterogeneities at a thinner (higher IS) than a thicker (lower IS) double layer as they move near the solid surface and find a local minima in the interaction energy. It would therefore be more difficult to remove colloids from local minima found under higher than lower IS conditions by changing the IS.

The primary objective of this research is to better understand the causes and implications of colloid/microbe retention hysteresis in porous media. The hypothesis that retention hysteresis occurs as a result of microscopic heterogeneity was tested by conducting transient IS transport experiments using porous media with different degrees of cleaning to reduce chemical impurities and surface roughness. If retention hysteresis occurs on unclean sand but not on clean sand, then hysteresis was due to the microscopic heterogeneities removed during cleaning. A secondary objective was to clarify the nature and reversibility of the adhesive interaction for colloids and microbes in porous media with changes in IS. In particular, secondary minimum interactions are expected to be reversible with changes in IS, whereas the reversibility of adhesive interactions due to heterogeneity will depend on the IS and the relative size of the heterogeneity and colloid/microbe. Knowledge of the nature and reversibility of the adhesive interaction is needed to predict the transport and fate of colloids and microbes in the environment.

2. Materials and methods

Ottawa sand that had a median grain diameter of 360 μm and a coefficient of uniformity of 1.88 was used in the transport studies. Ottawa sand is a natural aquifer material that is reported to consist of 99.8% SiO_2 (quartz) and trace amounts of metal oxides and clays. A salt cleaning procedure was employed to remove kaolinite clay from the sand surfaces (Bradford and Kim, 2010), namely (i) a 400-g sample of sand was placed on a sieve and flushed with deionized (DI) water; and (ii) the sieve and sand was immersed into 500 mM NaCl solution for 1 h and then flushed with DI water. This step was repeated until the optical density at 600 nm of the effluent DI water achieved an acceptable level. As a final cleaning step, the sand was added to excess DI water and sonicated for 1 h followed by an additional DI water rinse.

To reduce the amount of metal oxides, organic matter, and surface roughness an additional acid cleaning treatment (Redman et al., 2004) was applied to the salt treated sand. This procedure consisted of twice rinsing and overnight storage of the salt treated sand in 12 N hydrochloric acid (denoted as salt + acid treated sand). The sand mixture was then rinsed with DI water until the rinse water pH was equal to that of the DI water, and then the sand was re-hydrated by boiling in DI water for at least 1 h. The influence of the salt + acid treatment on the surface roughness of the finest portion (fraction retained on a #50 sieve) of the sand was assessed by measuring the BET surface area by Krypton (1100 ppm) adsorption (Quantachrome Corp., Syosset, NY) before and after acid treatment. Changes in the chemical properties of the finest portion of the sand were assessed by measuring concentrations of Ca, Mg, Al, and Fe in the HCl rinse using an inductively coupled plasma atomic emission spectrograph (Optima 3000, Dual View, PerkinElmer, Covina, CA).

Transport studies were conducted using 0.1 and 1.1 μm carboxyl modified latex (CML) colloids (Molecular Probes, Eugene, OR), coliphage φX174, and E. coli D21g. These colloids/microbes were suspended in various solutions of NaCl in DI water with its pH adjusted to 10 using 1.7 mM of Na_2CO_3 and 1.7 mM of $NaHCO_3$. Four IS levels were considered in these experiments, namely, 6, 31, 56, and 106 mM. To eliminate the secondary minimum, DI water at pH = 5.8 and IS = 0 was used as a final eluting solution. The pH of 10 was selected for transport experiments to yield highly unfavorable conditions that are known to produce hysteresis in the retention of colloids in the Ottawa sand (Torkzaban et al., 2010). The zero point of charge for quartz sand is between pH 2–3 (Sposito, 2008). However, the most common source of surface charge heterogeneity in natural aquatic environments is Fe and Al oxyhydroxides, which are amphoteric minerals with relatively high points of zero charge (Parks, 1965). For example, the zero point of charge of Fe oxide minerals ranges from pH 7.5–9. Consequently, quartz and iron oxides possess a net negative charge at pH 10, and any attractive electrostatic interactions between the colloids/microbes and porous medium are expected to be minimized at this pH. Lower pH conditions were not considered because iron oxides will be more positively charged and favorable for attachment. However, it should be mentioned that other researchers have observed significant amounts of colloid release with reductions in solution IS at lower pH (6.8–7.3) conditions (Lenhart and Saiers, 2003; Tosco et al., 2009).

The CML colloids were fluorescent with excitation at 505 nm and emission at 515 nm. The manufacturer reported values of the CML colloid size (0.1 or 1.1 μm in diameter), shape (spherical), density (1.05 g cm^{-3}), and hydrophobicity (hydrophilic). The input concentrations (C_o) for 0.1 and

1.1 μm CML colloids were 3E10 and 3E7 N_c mL^{-1} (where N_c denotes number of colloids), respectively. Average (three measurements) colloid concentrations reported herein were determined using a Turner Quantech Fluorometer (Barnstead/Thermolyne, Dubuque, IA) and reproducibility was typically within 1% of C_o.

Coliphage φX174 is a spherical, single stranded DNA coliphage that is 27-nm in diameter and has an isoelectric point of 6.6 (Dowd et al., 1998). This coliphage is considered to be a relatively conservative indicator for human virus transport because it is environmentally stable and has low hydrophobicity (Schijven and Hassanizadeh, 2000). The φX174 host bacterium, *E. coli* CN-13 (ATCC 700609), was incubated in trypticase soy broth for 18 h at 37 °C. Coliphage *φX174* was then added to this broth culture and allowed to propagate overnight. The host was then removed from the suspension containing *φX174* by centrifugation at 17,329×*g* for 10 min. The concentrated suspension of *φX174* was subsequently diluted in a desired electrolyte solution to achieve a C_o for φX174 of 7.5E6 to 1E7 N_c mL^{-1} for transport studies.

The concentration of φX174 in influent, effluent, and soil solution was determined using the double agar overlay Method 1601 (USEPA, 2001) with bacterial host *E. coli* CN-13. In brief, 1 mL of log phase host culture and 1-mL of sample were added to borosilicate test tubes (Thermo Fisher Scientific, Waltham, MA) containing 4 mL of trypticase soy agar (TSA) (BD Diagnostic Systems, Sparks, MD) supplemented with 1% nadidixic acid (Sigma-Aldrich, St. Louis, MO). The mixture was poured onto sterilized 100 by 15 mm plastic Petri plates (Thermo Fisher Scientific, Waltham, MA) and allowed to solidify for 15 min, after which they were inverted and incubated for 16 h at 37 °C. The number of plaque forming units (PFU) in the plates was determined by counting the plaque density under a darkfield colony counter (Leica, Buffalo, NY). All coliphage assays were run in duplicate and diluted as necessary. The value of C_o was measured six times during the course of a transient transport experiment to assess measurement reproducibility and the potential for aqueous phase inactivation. The standard deviation of these measurements was 13.1% of C_o and no systematic decrease in C_o was observed with time (little inactivation).

Escherichia coli D21g is gram-negative, nonmotile bacterial strain that produces minimal amounts of lipopolysaccharides (LPS) (Gmeiner and Schlecht, 1980; Walker et al., 2004) and extra-cellular polymeric substances (EPS) (Razatos et al., 1998). The effective diameter of D21g is 1.84 μm (Walker et al., 2004). A preculture of *E. coli* D21g was prepared by inoculating 5 mL of Luria–Bertani broth (LB Broth, Fisher Scientific, Fair Lawn, NJ) that had been supplemented with 0.03 mg/L gentamycin (Sigma, St. Louis, MO). The preculture was incubated on a rotary shaker overnight (12–18 h) at 37 °C and then added to 200 mL LB liquid media containing 0.03 mg/L gentamycin and incubated at 37 °C until reaching mid-exponential growth phase. The bacterial suspension was centrifuged to separate whole cells from the growth medium. The supernatant was decanted and the pellet was resuspended. To ensure that all traces of the growth medium were removed, the process of centrifuging, decanting, and resuspension was repeated three times before diluting the concentrated suspension into the desired electrolyte solution. Influent, effluent, and soil solution concentrations of *E. coli* D21g were determined using a spectrophotometer (Unico UV-2000, United Products & Instruments, Dayton, NJ) at a wavelength of 600 nm and a calibration curve. The optical density at 600 nm of the influent cell suspension was 0.2, and reproducibility was within 1% of C_o.

The zeta potential of these colloids/microbes in the various solution chemistries (Table 1) was calculated from experimentally measured electrophoretic mobilities using a ZetaPALS instrument (Brookhaven Instruments Corporation, Holtsville, NY) and the Smoluchowski equation. The zeta potential of the salt and salt + acid treated sands (Table 1) was determined from measured streaming potentials as a function of pH and IS using an Electro Kinetic Analyzer (Anton Paar GmbH, Graz, Austria) equipped with a cylindrical cell. A scanning electron microscope (XL30-FEG, Philips, Eindhoven, The Netherlands) was used to examine the surface roughness on salt and salt + acid treated sand.

The total interaction energy of the 0.1 and 1.1 μm CML colloids, φX174, and *E. coli* D21g upon approach to a sand under the various solution chemistries (pH = 10, and IS = 6, 31, 56, and 106 mM) was calculated (Table 1) using Derjaguin–Landau–Verwey–Overbeek (DLVO) theory and a sphere-plate assumption (Derjaguin and Landau, 1941; Verwey and Overbeek, 1948). Electrostatic double layer interactions were quantified using the expression of Hogg et al. (1966) using zeta potentials in place of surface potentials. The retarded London–van der Waals attractive interaction force was determined from the expression of Gregory (1981). Values of the Hamaker constant used in these calculations were 4.04E−21 J (Bergendahl and Grasso, 1999), 4E-21 J (Penrod et al., 1996), and 6.5E−21 J (Rijnaarts

Table 1
Zeta potentials and DLVO interaction energy parameters.

Colloid cleaning	Ionic strength (mM)	Sand zeta potential (mV)	Colloid zeta potential (mV)	Energy barrier (*kT*)	Depth of secondary energy minimum (*kT*)
1.1 μm CML salt	6	−71	−103.6	4790	0.2
	31	−46	−70.9	770	1.4
	56	−35	−62.1	309	2.7
	106	−27	−41.9	61	6.0
1.1 μm CML salt + acid	6	−55	−103.6	2574	0.2
	31	−41	−70.9	677	1.4
	56	−33	−62.1	289	2.8
	106	−28	−41.9	65	5.9
0.1 μm CML salt	6	−71	−64.2	203	0.0
	31	−46	−50.2	49	0.1
	56	−35	−40.0	18	0.3
	106	−27	−37.9	5	0.6
0.1 μm CML salt + acid	6	−55	−64.2	156	0.0
	31	−41	−50.2	44	0.1
	56	−33	−40.0	16	0.3
	106	−28	−37.9	5	0.6
D21g salt	6	−71	−52.9	3850	0.7
	31	−46	−42.2	1473	4.7
	56	−35	−33.5	654	9.9
	106	−27	−18.0	63	25.7
φX174 salt	6	−71	−28.0	19	0.01
	31	−46	−4.7	NB	–
	56	−35	−5.7	NB	–
	106	−27	−2.6	NB	–

NB, no barrier to attachment.

et al., 1995) for CML colloids, φX174, and *E. coli* D21g, respectively.

A schematic of the experimental setup and details on the procedures and protocols for obtaining the breakthrough curves (BTCs) and retention profiles (RPs) in the saturated packed column (15 cm long and 4.8 cm inside diameter) experiments are given by Bradford et al. (2002 and 2007). Column properties were relatively constant and included the porosity ($\varepsilon = 0.29–0.36$), the column length ($L_c = 11.2–13.0$ cm), and the Darcy velocity ($q = 0.09–0.12$ cm min^{-1}). The pulse duration for the 0.1 and 1.1 μm CML colloids was 160 min, for D21g it was 75 min, and for φX174 it was 140–180 min.

Transport experiments were carried out in three phases. First, several pore volumes of colloid/microbe suspension were introduced into the column at a constant rate (phase 1). Second, electrolyte solution was applied to the column at the same flow rate and IS as in the first phase until the effluent colloid/microbe concentration returned to a baseline level (phase 2). Finally, the influent IS was lowered in several steps to study mobilization/release (phase 3). After changing the IS in each step, the column was flushed with a lower IS solution until the change in effluent concentration was minimal. Effluent samples were collected during the transport experiment at selected intervals using a fraction collector and then the effluent samples were analyzed for colloid/microbe concentration as described above. The colloid/microbe mass recovery (%) was calculated as the ratio of the amount of eluted colloids/microbes during all three stages to the amount injected (Table 2).

Following recovery of the BTC the amount of colloids/microbes that were retained in the sand was determined (Table 2). The saturated sand was carefully excavated into tubes containing excess DI water. The tubes were slowly shaken for 15 min, and the concentration of the colloids in the excess aqueous solution (C_s) was determined as described above. The volume of solution (V_w) and mass of sand (m_s) in the tube was determined from the mass balance, and the recovery was quantified as $C_s V_w / m_s$. It should be mentioned that the focus of this research is on the colloid and microbe release during phase 3, and the RPs were strongly influenced by this release behavior. Consequently, only the total amount of 0.1 and 1.1 μm CML and ϕX174 that were recovered in the sand is reported in this work. Conversely, the amount of *E. coli* D21g retained in the sand could not be reliably determined using the spectrometer readings because of interference from sand particles.

Transport experiments for 0.1 and 1.1 μm CML, *E. coli* D21g, and ϕX174 were replicated for the initial IS = 106 mM condition. Mass balance results for colloid and microbe transport experiments are provided in Tables 2 and 3, respectively. Replicate column experiments conducted under the same experimental conditions (suspension and sand batch) exhibited good reproducibility. Differences in the replicate column experiments were more pronounced when using a new suspension and batch of sand, presumably due to slight variations in colloidal properties and/or sand cleaning. However, replicate transport experiments did exhibit the same qualitative trends, and similar interpretations and conclusions were derived from this data.

Table 2
Mass balance results from colloid transport experiments on salt and salt + acid treated sand.

Colloid cleaning	Initial IS (mM)	Breakthrough (%)								
		Transient IS (mM)								
		106	56	31	6	DI	FI[b]	M_{eff}[c]	M_s[d]	M_t[e]
1.1 μm CML salt	6	–	–	–	97.0	0.3	0.2	97.5	0.4	97.9
	31	–	–	90.0	1.3	3.3	0.4	95.0	1.3	96.3
	56	–	81.0	1.4	3.7	8.4	0.7	95.2	1.8	97.0
	106	24.5	3.3	4.5	15.5	35.5	2.1	85.4	7.9	93.3
	106[a]	21.6	9.1	8.5	17.2	35.6	ND	92.0	ND	ND
1.1 μm CML salt + acid	6	–	–	–	97.0	0.9	0.2	98.1	0.8	98.9
	31	–	–	94.2	1.2	3.5	0.3	99.2	0.9	100.0
	56	–	78.8	1.4	4.5	13.4	0.6	98.7	1.7	100.5
	106	58.2	2.2	2.8	10.1	23.3	0.6	97.2	2.3	99.9
	106[a]	33.6	3.1	2.8	13.6	21.9	ND	75.0	ND	ND
0.1 μm CML salt	6	–	–	–	97.6	0.5	0.4	98.5	0.3	98.9
	31	–	–	90.3	0.9	1.4	0.5	93.1	1.9	95.1
	56	–	61.1	1.7	2.0	6.7	1.0	72.5	7.8	80.3
	106	2.3	1.9	3.9	5.3	22.1	1.7	37.2	21.8	58.9
	106[a]	2.6	1.1	1.3	7.1	28.9	ND	41.0	ND	ND
0.1 μm CML salt + acid	6	–	–	–	99.5	0.8	0.2	100.5	0.4	100.9
	31	–	–	96.3	1.3	1.7	0.3	99.6	0.9	100.5
	56	–	89.9	1.4	1.6	3.0	0.5	96.4	2.0	98.3
	106	73.3	1.9	2.1	3.1	6.0	0.8	87.2	4.1	91.4
	106[a]	71.8	1.9	2.5	10.3	8.5	ND	95.0	ND	ND

ND, not determined.
[a] Replicate experiment.
[b] Flow interruption.
[c] Mass balance for effluent.
[d] Mass balance for sand.
[e] Total mass balance.

Table 3
Mass balance results from microbe transport experiments on salt treated sand.

Microbe	Initial IS (mM)	Breakthrough (%)					
		Transient IS (mM)					
		106	56	31	6	DI	M_{eff}[b]
D21g	6	–	–	–	87.1	4.8	91.9
	31	–	–	72.5	3.1	11.4	87.0
	56	–	66.1	2.7	4.0	9.7	82.5
	106	50.8	3.3	4.1	6.2	7.8	72.2
	106[a]	37.1	1.0	1.0	7.5	8.6	55.2
φX174	6	–	–	–	82.5	0.002	82.5
	106	54.4	0.4	0.4	1.3	1.6	58.1
	106[a]	80.7	0.4	2.3	0.5	1.2	85.1

[a] Replicate experiment.
[b] Mass balance for effluent.

3. Results and discussion

3.1. Characterization of colloids, microbes, and sand

Table 1 shows measured zeta potentials for 0.1 and 1.1 μm CML colloids, φX174, *E. coli* D21g, salt treated sand, and salt + acid treated sand for the various IS conditions, as well as the associated DLVO interaction energy parameters. Unfavorable conditions are predicted for 0.1 and 1.1 μm CML colloids and *E. coli* D21g at the various IS, and diffusion over the energy barriers into the primary energy minimum is unlikely based on considerations of the Maxwellian kinetic energy distribution (Shen et al., 2007). In contrast, favorable attachment conditions are predicted for φX174 at IS of 31, 56, and 106 mM, and a minor energy barrier and secondary minimum are predicted at IS of 6 mM. The height of energy barriers decreased with IS and decreasing colloid/microbe size, whereas the depth of the secondary minimum increased with IS and colloid/microbe size.

DLVO calculations indicate little difference in the adhesive interaction for a particular CML colloid at a given IS on salt and salt + acid treated sands. However, it should be emphasized that these zeta potentials and interaction energies only reflect mean values of the colloids/microbes on the solid water interface (SWI) and do not account for the influence of microscopic heterogeneity due to surface roughness and adsorbed multivalent cations. SEM images for salt and salt + acid treated sand are presented in Fig. 1. The degree of surface roughness on the salt + acid treated sand appears to be slightly decreased in comparison to that of the salt treated sand. Similarly, measurement of the BET surface area on the finer portion of the salt and salt + acid treated sand was measured to be 560 and 450 $cm^2\ g^{-1}$, respectively. This information indicates that the acid treatment reduced the BET surface area by 19.6%. Analyses of the major cations in the acid rinse further revealed the recovery of iron (12.3 μg of Fe per gram of sand), and trace amounts of Al and Ca. Consequently, the acid treatment reduced the amount of physical (surface roughness) and chemical (iron oxide) heterogeneity on the salt + acid treated sand.

3.2. Transport and retention of CML colloids

Breakthrough and release curves for 1.1 μm CML colloids in salt (Fig. 2a) and salt + acid (Fig. 2b) treated 360 μm sand are shown in Fig. 2 for the various IS conditions. Corresponding mass balance information is presented in Table 2. In contrast to DLVO predictions shown in Table 1, Fig. 2 demonstrates a decrease in the amount of colloid retention on the salt + acid treated sand in comparison to the salt treated sand. This result suggests an insensitivity of the mean streaming potential and associated DLVO predictions to microscopic heterogeneities on the sand surface that may arise from zones of weathering that are associated with incomplete removal of kaolinite, molecular-level structural defects, charge variation of hydroxyl groups, and the presence of metal oxides, cations, and organics on silica surfaces (Ryan and Elimelech, 1996; Song et al., 1994; Torkzaban et al., 2012; Tufenkji and Elimelech, 2005; Vaidyanathan and Tien, 1991).

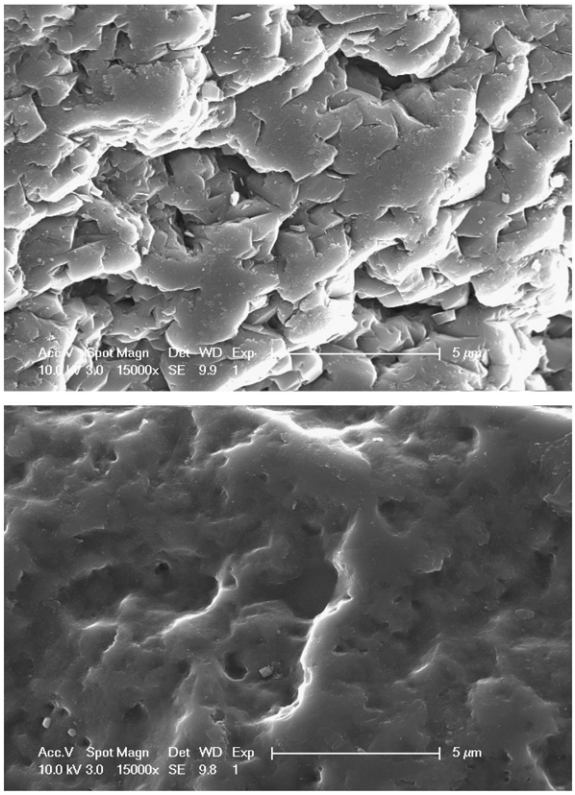

Fig. 1. SEM images of salt treated (top) and salt + acid (bottom) treated Ottawa sand.

Step reductions in IS shown in Fig. 2 produced 1.1 μm CML release under all conditions. This observation indicates that colloid immobilization and release were controlled by a balance of applied hydrodynamic and resisting adhesive torques that varied spatially with pore space geometry and microscopic heterogeneity, respectively (Bradford and Torkzaban, 2008; Bradford et al., 2011a; Torkzaban et al., 2010). The amount of colloid release was dependent on the sand cleaning procedure and the solution chemistry sequence. In general, relatively low amounts of colloid release occurred when the IS was decreased from 106 to 6 mM. In contrast, significant amounts of colloid release were observed when the IS was further reduced from 6 mM to DI water. These observations occurred for both salt and

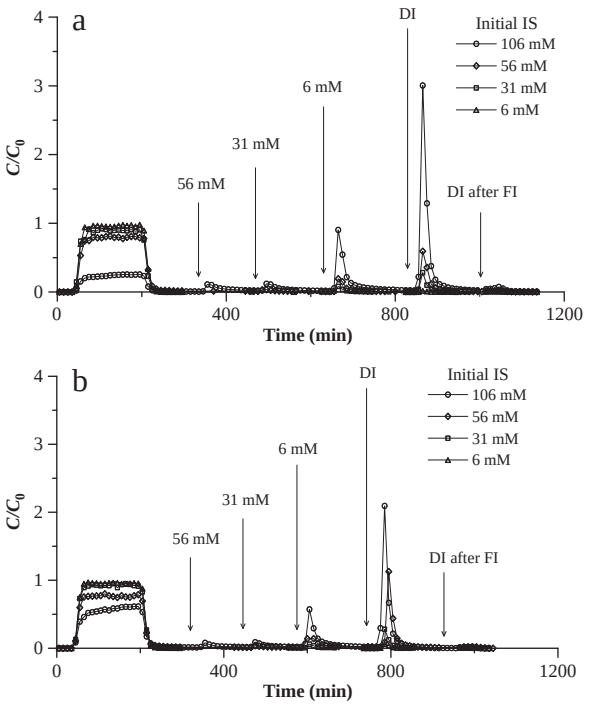

Fig. 2. Breakthrough and release curves for 1.1 μm CML colloids on salt (a) and salt + acid (b) treated sand at different initial IS conditions. Here the normalized effluent concentration (C/C_o, where C and C_o are the effluent and influent concentrations, respectively) is plotted as a function of time. The sequence of the transient experiments was: (i) deposition of colloids in the column during phase 1; (ii) elution with the same electrolyte solution (without colloids) during phase 2; and (iii) the eluting solution IS was lowered in several steps indicated on the figure during phase 3. Other experimental conditions are summarized in Tables 1–2 and the text.

salt + acid treated sands and indicate a relative insensitivity to decreases in IS until the double layer thickness was fully expanded.

To better help understand these processes, Fig. 3 presents effluent mass balance information from Table 2 for 1.1 μm colloids in terms of retention hysteresis with IS; i.e., different amounts of retention occur at the same IS conditions. The arrows indicate the direction of the IS change, with arrows facing to the right indicating results obtained during initial deposition (phase 1) and eluting (phase 2) phases, whereas those facing to the left were for release with step changes in eluting solution IS (phase 3). Several hypotheses have been proposed in the literature to explain retention hysteresis as discussed in the Introduction. Data presented in Fig. 3 allows us to examine these hypotheses in greater detail. Hysteresis in retention of 1.1 μm colloids was much more prevalent in the salt than the salt + acid cleaned sand. This indicates that microscopic heterogeneity is playing a dominant role in creating retention hysteresis in the salt treated sand for 1.1 μm colloids. Specifically, the number of local minima in the interaction energy that contributes to colloid retention and release changes with the IS history. Similarly, simulation of the transient transport data shown in Fig. 2a revealed that a greater fraction of the solid surface area contributed to retention as the IS increased (Bradford et al., in review).

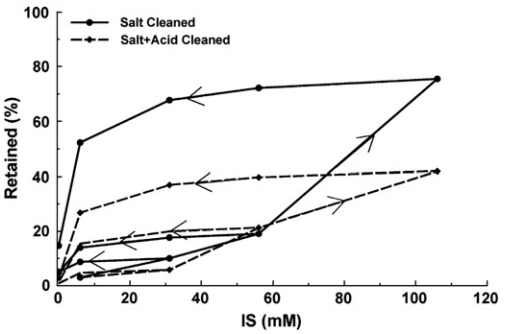

Fig. 3. A summary of the retention data during the transient IS experiments for the 1.1 μm CML colloids in salt and salt + acid treated sand. Here the percentages of retained colloids are plotted as a function of the solution IS history. The arrows indicate the direction of the IS change, with arrows facing to the right for phases 1 and 2 and to the left for phase 3.

Duffadar and Davis (2007) used the grid surface integration (GSI) technique to calculate the interaction energy for colloids near a heterogeneously charged solid surface. To interpret the influence of microscopic chemical heterogeneity on colloid interactions an electrostatic zone of influence (ZOI) was defined which is proportional to the square root of the product of the colloid radius and the Debye length. GSI calculations indicated that spatial variations in charge produce less deviation from the mean interaction when the ZOI was large (Duffadar and Davis, 2007). For 1.1 μm colloids the radius of the ZOI is proportional to 2.5, 0.93, 0.80, and 0.68 nm when the IS equals 6, 31, 56, and 106 mM, respectively. Table 2 provides mass balance information for the 1.1 μm colloids, including the amount recovered from the sand in DI water during the excavation phase of the experiment. Very good mass balance was achieved with the 1.1 μm colloids on both salt (93.3–97.9%) and salt + acid (98.9–100.5%) treated sand, indicating that almost all the 1.1 μm colloids interacted reversibly with the SWI. This information suggests that the ZOI was sufficiently large for the 1.1 μm colloids to produce an adhesive interaction that was similar to a reversible secondary minimum.

Other GSI calculations indicated that microscopic variations in charge can cause significant deviations from the mean interaction energy that result in local minima which were favorable for retention when the ZOI was small (Duffadar and Davis, 2007). For 0.1 μm colloids the radius of the ZOI is proportional to 0.79, 0.29, 0.25, and 0.22 nm when the IS equals 6, 31, 56, and 106 mM, respectively. Consequently, the above information indicates that 0.1 μm colloids are expected to be more sensitive to microscopic heterogeneities than the 1.1 μm colloids at similar IS conditions because of their smaller ZOI. Furthermore, the influence of microscopic heterogeneities is expected to increase with IS (smaller ZOI) and on salt treated sand (greater amounts of microscopic surface roughness and chemical heterogeneity).

Additional column experiments were therefore conducted to better understand the role of microscope heterogeneities on the transport, retention, and release of 0.1 μm colloids. Breakthrough and release curves for 0.1 μm CML colloids in salt (Fig. 4a) and salt + acid (Fig. 4b) treated 360 μm sand are shown in Fig. 4 for the various IS conditions. Fig. 5 presents effluent mass balance information (Table 2) for 0.1 μm colloids in terms of retention

hysteresis with IS. Similarities and differences in the behavior of 0.1 and 1.1 μm CML colloids will be discussed below.

The transport, retention, and release of 0.1 μm colloids were sensitive to the solution IS and the sand cleaning treatment, similar to Figs. 2 and 3 for the 1.1 μm colloids. In brief, retention of 0.1 μm colloids (phases 1 and 2) increased with IS and for the salt treated sand as expected due to the smaller ZOI and greater amounts of microscopic heterogeneity, respectively. The amount of 0.1 μm colloid that was released during phase 3 increased as the IS decreased consistent with torque balance considerations. Colloid recovery from the sand (Table 2) was most pronounced in systems having the smallest ZOI during phases 1 and 2 (higher IS and smaller sized 0.1 μm colloid) and the greatest amounts of microscopic heterogeneity (salt treated sand). Hence, even a miniscule adhesive interaction from microscopic heterogeneity may have been sufficient to retain colloids after flushing with DI water, especially in low velocity regions such as grain-grain contacts and surface roughness locations.

Figs. 2–5 indicate some interesting differences for the 1.1 and 0.1 μm colloids in the salt treated sand. Comparison with 1.1 and 0.1 μm colloids at given IS conditions reveals that 0.1 μm colloids exhibited greater amounts of retention and more time-dependent (blocking) transport behavior (Table 2; Figs. 2a and 4a), lower amounts of release (Table 2; Figs. 2a and 4a), and more irreversible retention (Figs. 3 and 5). Simulation of the transient transport data shown in Figs. 2a and 4a revealed that a greater fraction of the solid surface area contributed to retention as the IS increased and the colloid size decreased (Bradford et al., in review). This surface area

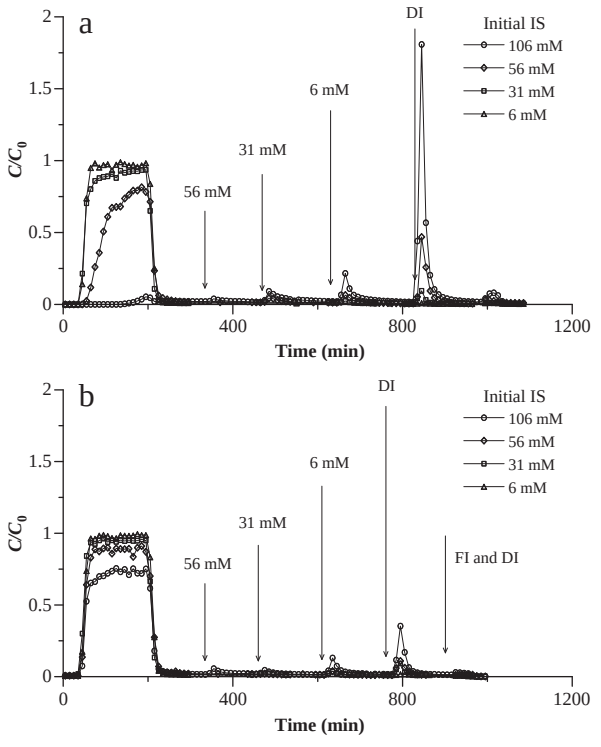

Fig. 4. Breakthrough and release curves for 0.1 μm CML colloids on salt (a) and salt + acid (b) treated sand at different initial IS conditions. Other experimental conditions are summarized in Tables 1–2 and the text.

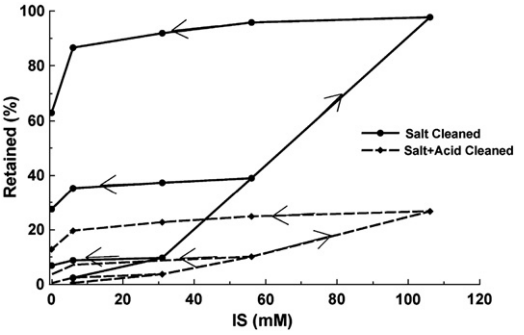

Fig. 5. A summary of the retention data during the transient IS experiments for the 0.1 μm CML colloids in salt and salt + acid treated sand.

fraction plays a critical role in determining the observed time-dependent (blocking) deposition behavior shown in Fig. 4a (Bradford et al., 2011b). Furthermore, all of the above observations are consistent with GSI calculations on microscopically heterogeneous surfaces that predict an increasing strength of interaction with increasing IS and decreasing colloid size (Duffadar and Davis, 2007).

The ZOI is much smaller for 0.1 than 1.1 μm colloids at a given IS. Consequently, only a relatively small fraction of the 0.1 μm colloids on salt treated sand interacted reversibility (similar to secondary minimum) and the remaining colloids strongly interacted with microscopic heterogeneities. Consistent with predicted trends in the ZOI, the total mass balance (Table 2) for 0.1 μm colloids on salt treated sand decreased as the IS increased (58.9–98.0%), and was significantly less than that for the 1.1 μm colloids (93.3–97.9%). It should be mentioned that differences in the reversibility of 1.1 and 0.1 μm colloids are also dependent on the applied hydrodynamic torque, which is proportional to the cube of the colloid radius as the separation distance goes to zero on a flat surface (e.g., Duffadar and Davis, 2008). On a rough surface the applied hydrodynamic torque is zero when the colloid radius is less than the height of the surface roughness (Vaidyanathan and Tien, 1991). Consistent with experimental observations, this implies much greater colloid release is expected for larger than smaller colloids under similar adhesive conditions.

The sand cleaning treatment had an especially large influence on the retention of the 0.1 μm colloids when the IS was 106, 56, and 31 mM (Fig. 5). In contrast, differences in the retention of the 1.1 μm CML colloids for the two cleaning treatments occurred only when the IS was 106 mM (Fig. 3). Apparently, the influence of the sand cleaning treatment was more pronounced as the IS increased and the colloid size decreased. The mean value of the secondary minimum increased with IS, but decreased with colloid size (Table 1). Hence, the secondary minimum cannot explain the observed behavior for the 0.1 μm colloids on the salt treated sand. Conversely, these trends are completely consistent with calculated values of the ZOI discussed above that decrease with increasing IS and decreasing colloid size.

Examination of Fig. 3 (1.1 μm colloids) and Fig. 5 (0.1 μm colloids) reveals that salt + acid treatment of the sand does not remove all of the retention hysteresis. Although the magnitude of colloid retention is quite different in salt and salt + acid

treated sands, the shape of the retention hysteresis curve exhibits many similarities. This observation suggests a similar origin for the retention hysteresis curves for both cleaning treatments. The salt + acid treatment reduces the amounts of metal oxides and surface roughness, but will not influence the incomplete removal of kaolinite, structural defects, and variation of charge of hydroxyl groups (Bohn et al., 1985; Vaidyanathan and Tien, 1991). Hence, retention hysteresis in the salt + acid treated sand likely occurred due to incomplete removal of the microscopic heterogeneities. Alternatively, surface charge heterogeneity of the colloid populations provides another viable explanation (Bolster et al., 1999; Li et al., 2004; Tufenkji and Elimelech, 2005). Charge heterogeneity on polystyrene latex particles has been measured and attributed to separation of ion-rich and ion-poor components of the polymer on the particle surface (Tan et al., 2005). It is possible that microscopic heterogeneity on both the SWI and colloids may be playing a role in the retention hysteresis of colloids in the salt + acid treated sand, although it is not feasible to separate these effects without additional information.

Comparison of the hysteresis curves for salt and salt + acid treated sand in Figs. 3 and 5 reveals an important difference. In contrast to the salt treated sand, greater amounts of colloid retention occurred for 1.1 (Fig. 3) than 0.1 (Fig. 5) μm colloids after reduction of the microscopic heterogeneity by acid treatment. DLVO theory predicts a greater depth of the secondary minimum for 1.1 than 0.1 μm colloids based on mean values of the zeta potentials (Table 1). This observation implies that the mean adhesive interaction (similar to secondary minimum) was dominating the deposition and release behavior of 1.1 and 0.1 μm colloids on the salt + acid treated sand after reduction in the amount of microscopic heterogeneity.

3.3. Transport and retention of microbes

The information presented above demonstrates the importance of microscopic heterogeneity on CML colloid retention and release. This section examines the influence of these same factors for several representative microorganisms, φX174 and *E. coli* D21g, during similar transport and release experiments on salt treated sand. Experiments on salt + acid treated sand were not conducted because the underlying retention and release mechanisms were found to be the same for CML colloids on salt and salt + acid treated sand, with only the magnitude of the retention changing with the cleaning treatment.

Fig. 6a and b presents breakthrough and release curves for *E. coli* D21g and φX174, respectively, on salt treated sand for the initial IS = 106 mM condition. The initial amount of retention was quite similar for φX174 and *E. coli* D21g at IS = 106 mM. This result is somewhat surprising because Table 1 indicates pronounced differences in the predicted strength of the DLVO interaction for φX174 (favorable conditions) and *E. coli* D21g (secondary minimum), and filtration theory predicts that the collector efficiency (η) is much larger for the smaller φX174 (η = 0.28) than for *E. coli* D21g (η = 0.02). Both of these factors imply greater amounts of retention for φX174 than for *E. coli* D21g when the IS = 106 mM. This finding is clearly not consistent with the observed data, and indicates that φX174 is experiencing unfavorable conditions even at IS = 106 mM. One potential explanation for this deviation is due to the inability of macroscopic zeta potentials to accurately describe adhesive interactions on microscopically heterogeneous surfaces (Kim et al., 2009) as has been demonstrated for the 1.1 and 0.1 μm CML colloids. In addition, the retention behavior of *E. coli* D21g and φX174 is expected to be even more complicated than CML colloids due to differences in shape (*E. coli* D21g is rod shaped), size, surface charge (Table 1), presence/absence of surface macromolecules and structures, and the potential of non-DLVO repulsive forces (e.g., steric and/or born repulsion).

A summary of the transient IS experiments for φX174 and *E. coli* D21g on salt treated sand is provided in Fig. 7 by presenting the retention hysteresis with IS. Retention hysteresis was observed for both φX174 and *E. coli* D21g when the IS of the eluting solution was decreased in a stepwise manner during phase 3. Step reductions in IS produce only low amounts of φX174 release, whereas a much greater percentage of the *E. coli* D21g was released under the same solution chemistry conditions. *E. coli* D21g was significantly more reversibly retained than φX174, and this trend is qualitatively consistent with the release behavior for 1.1 (Fig. 3) and 0.1 (Fig. 5) μm CML colloids, respectively. As discussed previously for CML colloids, these observations imply that φX174 was strongly, and largely

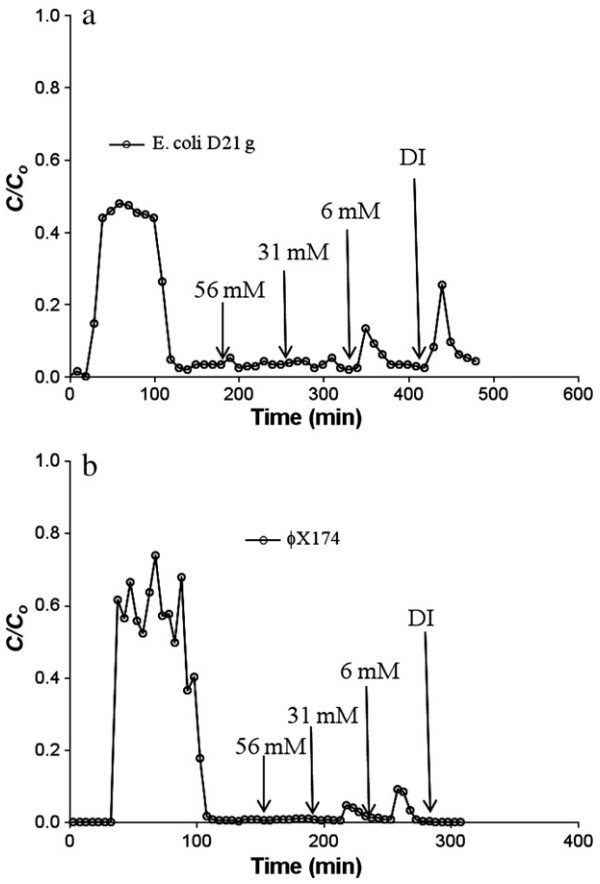

Fig. 6. Breakthrough and release curves for *E. coli* D21g (a) and φX174 (b) on salt treated sand for the initial IS = 106 mM condition.

irreversibly, interacting with heterogeneities that are similar or greater in size than the coliphage. However, it should be noted that *E. coli* D21g exhibited less reversibility in retention than either 1.1 (Fig. 3) or 0.1 (Fig. 5) μm CML colloids, and a direct comparison of microbes and CML colloids was not possible because of differences in the adhesive interactions (see the previous paragraph).

4. Conclusions

Studies were conducted to investigate the causes and implications of colloid and microorganisms retention hysteresis. The main conclusions from this study are as follows:

- Calculated DLVO interaction energies did not provide a good characterization of the adhesive interaction for colloids/microbes on the SWI because they considered only mean zeta potentials and neglected the influence of microscopic heterogeneities.
- The retention and release of colloids/microbes were strongly influenced by microscopic physical (surface roughness) and/or chemical (iron oxides) heterogeneities on the sand surfaces. Even a miniscule adhesive interaction from chemical heterogeneity was sufficient to retain colloids under highly unfavorable attachment conditions.
- Microscopic heterogeneities were the dominant cause for retention hysteresis of colloids and microorganisms, influencing the number and strength of local minima in the interaction energy that contributes to retention and release with changes in IS.
- Release of colloids/microbes was dependent on the relative size of the colloids/microbes to the heterogeneity, the Debye length, and the applied hydrodynamic torque.
- Smaller 0.1 μm CML colloids were more irreversibly retained in sand than 1.1 μm CML colloids because they experienced lower values of the applied hydrodynamic torque and greater depths in the local minima of the interaction energy near microscopic heterogeneities. Similarly, the larger *E. coli* D21g exhibited greater reversibility in retention than φX174. However, direct comparison of CML colloids and microbes was not possible due to differences in size, shape, and surface properties.
- CML retention and release were more consistent with mean interaction energies and hysteresis was minimized on salt + acid treated sand due to reduction in the amount of microscopic heterogeneities.

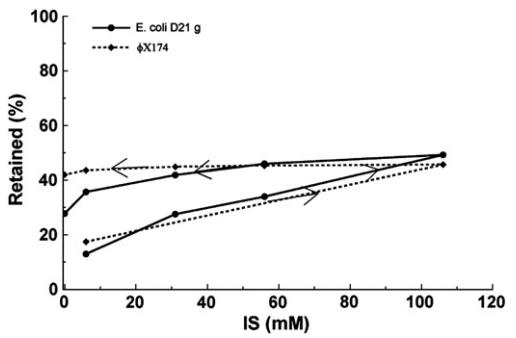

Fig. 7. A summary of the retention data during the transient IS experiments for φX174 and *E. coli* D21g on salt treated sand.

Acknowledgements

We would like to thank Lorena Altamirano for her help in conducting the transport experiments. This research was supported by the USDA, ARS, NP 214. The USDA is an equal opportunity provider and employer.

References

Adamczyk, Z., Siwek, B., Zembala, M., Belouschek, P., 1994. Kinetics of localized adsorption of colloid particles. Advances in Colloid and Interface Science 48, 151–280.
Bergendahl, J., Grasso, D., 1999. Prediction of colloid detachment in a model porous media: thermodynamics. AICHE Journal 45, 475–484.
Bohn, H.L., McNeal, B.L., O'Connor, G.A., 1985. Soil chemistry, 2nd ed. John Wiley & Sons, New York.
Bolster, C.H., Mills, A.L., Hornberger, G.M., Herman, J.S., 1999. Spatial distribution of deposited bacteria following miscible displacement experiments in intact cores. Water Resources Research 35, 1797–1807.
Bradford, S.A., Kim, H., 2010. Implications of cation exchange on clay release and colloid-facilitated transport in porous media. Journal of Environmental Quality 39, 2040–2046.
Bradford, S.A., Torkzaban, S., 2008. Colloid transport and retention in unsaturated porous media: a review of interface, collector, and pore scale processes and models. Vadose Zone Journal 7, 667–681.
Bradford, S.A., Yates, S.R., Bettahar, M., Šimunek, J., 2002. Physical factors affecting the transport and fate of colloids in saturated porous media. Water Resources Research 38, 1327, http://dx.doi.org/10.1029/2002WR001340.
Bradford, S.A., Torkzaban, S., Walker, S.L., 2007. Coupling of physical and chemical mechanisms of colloid straining in saturated porous media. Water Research 41, 3012–3024.
Bradford, S.A., Torkzaban, S., Wiegmann, A., 2011a. Pore-scale simulations to determine the applied hydrodynamic torque and colloid immobilization. Vadose Zone Journal 10, 252–261.
Bradford, S.A., Torkzaban, S., Simunek, J., 2011b. Modeling colloid transport and retention in saturated porous media under unfavorable attachment conditions. Water Resources Research 47, W10503, http://dx.doi.org/10.1029/2011WR010812.
Bradford, S.A., Torkzaban, S., Kim, H., Simunek, J., in review. Modeling colloid and microorganism transport and release with transients in solution ionic strength. Water Resources Research.
Derjaguin, B.V., Landau, L.D., 1941. Theory of the stability of strongly charged lyophobic sols and of the adhesion of strongly charged particles in solutions of electrolytes. Acta Physicochimica U.S.S.R. 14, 733–762.
Dowd, S.E., Pillai, S.D., Wang, S.Y., Corapcioglu, M.Y., 1998. Delineating the specific influence of virus isoelectric point and size on virus adsorption and transport through sandy soils. Applied and Environmental Microbiology 64, 405–410.
Duffadar, R.D., Davis, J.M., 2007. Interaction of micrometer-scale particles with nanotextured surfaces in shear flow. Journal of Colloid and Interface Science 308, 20–29.
Duffadar, R.D., Davis, J.M., 2008. Dynamic adhesion behavior of micrometer-scale particles flowing over patchy surfaces with nanoscale electrostatic heterogeneity. Journal of Colloid and Interface Science 326, 18–27.
Duffadar, R., Kalasin, S., Davis, J.M., Santore, M.M., 2009. The impact of nanoscale chemical features on micron-scale adhesion: Crossover from heterogeneity-dominated to mean field behavior. Journal of Colloid and Interface Science 337, 396–407.
Franchi, A., O'Melia, C.R., 2003. Effects of natural organic matter and solution chemistry on the deposition and reentrainment of colloids in porous media. Environmental Science and Technology 37, 1122–1129.
Gmeiner, J., Schlecht, S., 1980. Molecular composition of the outer membrane of Escherichia coli and the importance of protein–lipopolysaccharide interactions. Archives of Microbiology 127, 81–86.
Gregory, J., 1981. Approximate expression for retarded van der Waals interaction. Journal of Colloid and Interface Science 83, 138–145.
Hahn, M.W., Abadzic, D., O'Melia, C.R., 2004. Aquasols: on the role of secondary minima. Environmental Science and Technology 38, 5915–5924.
Hoek, E.M.V., Agarwal, G.K., 2006. Extended DLVO interactions between spherical particles and rough surfaces. Journal of Colloid and Interface Science 298, 50–58.
Hogg, R., Healy, T.W., Fuerstenau, D.W., 1966. Mutual coagulation of colloidal dispersions. Transactions of the Faraday Society 62, 1638–1651.

Johnson, P.R., Sun, N., Elimelech, M., 1996. Colloid transport in geochemically heterogeneous porous media: modeling and measurements. Environmental Science and Technology 30, 3284–3293.
Kalasin, S., Santore, M.M., 2008. Hydrodynamic crossover in dynamic microparticle adhesion on surfaces of controlled nanoscale heterogeneity. Langmuir 24, 4435–4438.
Kim, H.N., Bradford, S.A., Walker, S.L., 2009. Escherichia coli O157:H7 transport in saturated porous media: role of solution chemistry and surface macromolecules. Environmental Science and Technology 43, 4340–4347.
Kozlova, N., Santore, M.M., 2006. Micron-scale adhesion dynamics mediated by nanometer-scale surface features. Langmuir 22, 1135–1142.
Kozlova, N., Santore, M.M., 2007. Micrometer scale adhesion on nanometer-scale patchy surfaces: adhesion rates, adhesion thresholds, and curvature-based selectivity. Langmuir 23, 4782–4791.
Kuznar, Z.A., Elimelech, M., 2007. Direct microscopic observation of particle deposition in porous media: role of the secondary energy minimum. Colloids and Surfaces A: Physicochemical and Engineering Aspects 294, 156–162.
Lenhart, J.J., Saiers, J.E., 2003. Colloid mobilization in water-saturated porous media under transient chemical conditions. Environmental Science and Technology 37, 2780–2787.
Li, X., Scheibe, T.D., Johnson, W.P., 2004. Apparent decreases in colloid deposition rate coefficient with distance of transport under unfavorable deposition conditions: a general phenomenon. Environmental Science and Technology 38, 5616–5625.
Parks, G.A., 1965. Isoelectric points of solid oxides, solid hydroxides, and aqueous hydroxo complex systems. Chemistry Review 65, 177–198.
Penrod, S.L., Olson, T.M., Grant, S.B., 1996. Deposition kinetics of two viruses in packed beds of quartz granular media. Langmuir 12, 5576–5587.
Privman, V., Frisch, H.L., Ryde, N., Matijevic, E., 1991. Particle adhesion in model systems. Part 13.—Theory of multilayer deposition. Journal of the Chemical Society, Faraday Transactions 87, 1371–1375.
Razatos, A., Ong, Y.L., Sharma, M.M., Georgiou, G., 1998. Molecular determinants of bacterial adhesion monitored by atomic force microscopy. Proceedings of the National Academy of Sciences of the United States of America 95, 11059–11064.
Redman, J.A., Walker, S.L., Elimelech, M., 2004. Bacterial adhesion and transport in porous media: role of the secondary energy minimum. Environmental Science and Technology 38, 1777–1785.
Rijnaarts, H.H.M., Norde, W., Bouwer, E.J., Lyklema, J., Zehnder, A.J.B., 1995. Reversibility and mechanism of bacterial adhesion. Colloids and Surfaces B: Biointerfaces 4, 5–22.
Russel, W.B., Saville, D.A., Schowlter, W.R., 1989. Colloidal Dispersions. Cambridge University Press, Cambridge.
Ryan, J.N., Elimelech, M., 1996. Colloid mobilization and transport in groundwater. Colloids and Surfaces A: Physicochemical and Engineering Aspects 107, 1–56.
Schijven, J.F., Hassanizadeh, S.M., 2000. Removal of viruses by soil passage: overview of modeling, processes, and parameters. Critical Reviews in Environmental Science and Technology 30, 49–127.
Shen, C., Li, B., Huang, Y., Jin, Y., 2007. Kinetics of coupled primary- and secondary-minimum deposition of colloids under unfavorable chemical conditions. Environmental Science and Technology 41, 6976–6982.
Song, L., Johnson, P.R., Elimelech, M., 1994. Kinetics of colloid deposition onto heterogeneously charged surfaces in porous media. Environmental Science and Technology 28, 1164–1171.
Sposito, G., 2008. The chemistry of soils. Oxford Univ. Press, New York.
Tan, S., Sherman, R.L., Qin, D., Ford, W.T., 2005. Surface heterogeneity of polystyrene latex particles determined by dynamic force microscopy. Langmuir 21, 43–49.
Taneda, S., 1979. Visualization of separating Stokes flows. Journal of the Physical Society of Japan 46, 1935–1942.
Torkzaban, S., Bradford, S.A., Walker, S.L., 2007. Resolving the coupled effects of hydrodynamics and DLVO forces on colloid attachment to porous media. Langmuir 23, 9652–9660.
Torkzaban, S., Tazehkand, S.S., Walker, S.L., Bradford, S.A., 2008. Transport and fate of bacteria in porous media: coupled effects of chemical conditions and pore space geometry. Water Resources Research 44, W04403, http://dx.doi.org/10.1029/2007WR006541.
Torkzaban, S., Kim, H.N., Simunek, J., Bradford, S.A., 2010. Hysteresis of colloid retention and release in saturated porous media during transients in solution chemistry. Environmental Science and Technology 44, 1662–1669.
Torkzaban, S., Wan, J., Tokunaga, T.K., Bradford, S.A., 2012. Impacts of bridging complexation on the transport of surface-modified nanoparticles in saturated sand. Journal of Contaminant Hydrology 136–137, 86–95.
Tosco, T., Tiraferri, A., Sethi, R., 2009. Ionic strength dependent transport of microparticles in saturated porous media: modeling mobilization and immobilization phenomena under transient chemical conditions. Environmental Science and Technology 43, 4425–4431.
Tufenkji, N., Elimelech, M., 2005. Breakdown of colloid filtration theory: role of the secondary energy minimum and surface charge heterogeneities. Langmuir 21, 841–852.
USEPA, 2001. Manual of methods for virology. USEPA Rep. 600/4–84/013 (N16. U.S. Gov. Print. Office, Washington, DC.
Vaidyanathan, R., Tien, C., 1991. Hydrosol deposition in granular media under unfavorable surface conditions. Chemical Engineering Science 46, 967–983.
Verwey, E.J.W., Overbeek, J.T.G., 1948. Theory of the stability of lyophobic colloids. Elsevier, Amsterdam.
Walker, S.L., Redman, J.A., Elimelech, M., 2004. Role of cell surface lipopolysaccharides in Escherichia coli K12 adhesion and transport. Langmuir 20, 7736–7746.
Wan, J.M., Tokunaga, T.K., 2002. Partitioning of clay colloids at air–water interfaces. Journal of Colloid and Interface Science 247, 54–61.